# Far-infrared spectral studies of magnesium and aluminum co-substituted lithium ferrites

K B MODI, J D GAJERA, M P PANDYA, H G VORA and H H JOSHI
Department of Physics, Saurashtra University, Rajkot 360 005, India
E-mail: kunalbmodi2003@yahoo.com

**Abstract.** Polycrystalline $Mg_xAl_{2x}Li_{0.5(1-x)}Fe_{2.5(1-x)}O_4$ ($x = 0.0, 0.2, 0.5, 0.6$ and $0.7$) ferrites were prepared by standard ceramic method, and characterized by X-ray diffraction and infrared absorption spectroscopy. The spectra show two significant absorption bands in the wave number range of 400–1000 cm$^{-1}$ arising from interatomic vibrations in the tetrahedral and octahedral coordination compounds. The decrease in intensity and increase in broadness of bands with concentration ($x$) are explained on the basis of cation distribution. The force constants and bulk modulus are found to decrease with Mg–Al content ($x$) which suggested weakening of interatomic bonding. An alternate method for the determination of bulk modulus, longitudinal and transverse velocities is suggested. The magnetic and electrical properties of these compounds are explained in the light of structural and optical properties.

**Keywords.** Ferrites; far-infrared spectra; interatomic bonding.

**PACS Nos**   **75.50.G; 61.10.F; 78.30; 35.20.D**

## 1. Introduction

Far-infrared absorption spectroscopy has been used to study the occurrence of various absorption bands in the spectra and analysed on the basis of different cations present on tetrahedral (A-) and octahedral (B-) sites of the spinel lattice [1–11]. It is also used to determine the local symmetry in crystalline solids [2], non-crystalline solids [3], ordering phenomenon in spinels [4,5], presence/absence of $Fe^{2+}$ ions [6,7] and also to determine force constants for A- and B-sites [1,8]. The detailed analysis of IR spectra with precise crystallographic knowledge helps to determine elastic moduli, Debye temperature, molar heat capacity, longitudinal and shear velocities but this requires a long chain of complicated mathematical simulations [1].

In the present work, we report the analysis on infrared spectroscopic study of $Mg_xAl_{2x}Li_{0.5(1-x)}Fe_{2.5(1-x)}O_4$ spinel ferrite system with $x = 0.0, 0.2, 0.5, 0.6$ and $0.7$. This work is a continuation of our work on magnetic [12] and structural [13] properties of the $Mg_xAl_{2x}Li_{0.5(1-x)}Fe_{2.5(1-x)}O_4$ system. The force constants are

calculated and an alternate method for the determination of bulk modulus, longitudinal and shear velocities is suggested. The magnetic and electrical properties of the system are explained on the basis of structural and optical properties. The motivation for co-substitution of $Mg^{2+}$ and $Al^{3+}$ in $Li_{0.5}Fe_{2.5}O_4$ stems from the possibility of studying the influence of coexistence of mono-, di- and tri-valent cations on infrared spectrum.

## 2. Experimental details

Five samples of $Mg^{2+}$ and $Al^{3+}$ co-substituted $Li_{0.5}Fe_{2.5}O_4$ with general formula $Mg_xAl_{2x}Li_{0.5(1-x)}Fe_{2.5(1-x)}O_4$ ($x = 0.0, 0.2, 0.5, 0.6$ and $0.7$) were prepared by the usual double sintering ceramic technique. The starting materials were MgO, $Al_2O_3$, $Li_2CO_3$ and $Fe_2O_3$ all 99.3% pure and supplied by E Merck. The oxides were mixed thoroughly in stoichiometric proportion to yield the desired composition and wet ground. The mixture was dried and pressed into pellets. These pellets were calcined at 950°C for 24 h. In the final sintering process, the samples were kept at 1150°C for 24 h and slowly cooled to room temperature at the rate of 2°C/min. The final density of the products was found to be about 83% of the X-ray density. The X-ray diffraction patterns for all the compositions were recorded at 300 K with a Philips (model: PM 9220) diffractometer using $FeK\alpha$ radiation. The infrared spectra for all the compositions at 300 K were recorded in the wave number range of 400–1000 $cm^{-1}$. For the present samples, BRUKER IFS 66V FT–IR spectrometer was used to carry out the infrared spectroscopic studies in KBr medium.

## 3. Results and discussion

The room temperature (300 K) X-ray diffraction pattern of each composition corresponded to well-defined crystalline fcc phase and confirmed the spinel structure. The concentration dependence of lattice constant $a$ with an accuracy of $\pm 0.002$ Å determined from X-ray diffraction data is presented in table 1. The lattice constant gradually decreases with increasing $x$, obeying the Vegard's law [14]. The linear decrease in the lattice constant is due to the replacement of larger $Li^+$ (0.70 Å) and $Fe^{3+}$ (0.64 Å) ions by smaller $Al^{3+}$ (0.51 Å) ions in the $Mg_xAl_{2x}Li_{0.5(1-x)}Fe_{2.5(1-x)}O_4$ system. The X-ray density for each composition was calculated using the relation [15]:

$$\rho = ZM/Na^3,$$

where $Z$ is the number of molecules per unit cell ($Z = 8$) of the spinel lattice, $M$ is the molecular weight of the ferrite sample, $N$ is the Avogadro's number and $a$ is the lattice constant. The variation of X-ray density ($\rho$) with concentration ($x$) is shown in table 1. In the present case, X-ray density decreases in spite of the decrease in lattice constant with increasing $x$. This is due to the fact that, decrease in mass ($M$) overtakes the decrease in volume of the unit cell ($a^3$) in the system.

The oxygen positional parameter ($u$) for each composition was deduced from the value of $u$ for the two end members $Li_{0.5}Fe_{2.5}O_4$ ($x = 0.0$, $u = 0.260$ Å) and

**Table 1.** Lattice constant ($a$), X-ray density ($\rho$), oxygen positional parameter ($u$), site radii ($R_A$ and $R_B$) and force constants ($K_t$, $K_o$) for Mg–Al–Li–Fe–O system.

| Content ($x$) | $a$ (Å) $\pm 0.002$ Å | $\rho$ (g/cm$^3$) | $u$ (Å) | $R_A$ (Å) | $R_B$ (Å) | $K_t \times 10^5$ (dynes/cm) | $K_o \times 10^5$ (dynes/cm) |
|---|---|---|---|---|---|---|---|
| 0.0 | 8.370 | 4.691 | 0.2600 | 1.972 | 2.005 | 1.47 | 1.02 |
| 0.2 | 8.332 | 4.474 | 0.2604 | 1.963 | 1.995 | 1.34 | 0.91 |
| 0.5 | 8.275 | 4.095 | 0.2610 | 1.949 | 1.982 | 1.19 | 0.81 |
| 0.6 | 8.281 | 3.934 | 0.2612 | 1.951 | 1.983 | 1.21 | 0.77 |
| 0.7 | 8.234 | 3.848 | 0.2614 | 1.939 | 1.972 | 1.12 | 0.75 |

$MgAl_2O_4$ ($x = 1.0$, $u = 0.262$ Å) obtained from the literature [16,17] and tabulated in table 1. The X-ray diffraction data was further used to calculate the tetrahedral and octahedral site radii ($R_A$ and $R_B$). The site radii, $R_A$ and $R_B$, were calculated using the relations,

$$R_A = a(3)^{1/2}(\delta + 1/8),$$
$$R_B = a(3\delta^2 + 1/16 - \delta/2)^{1/2}, \tag{1}$$

where $\delta = u_{\text{system}} - u_{\text{ideal}}$, $u_{\text{system}} = $ oxygen parameter $= (u_1 + u_2)/2$ and $u_{\text{ideal}} = 0.250$ Å where $u_1$ and $u_2$ are oxygen parameters of the two end members of the system, respectively.

The values of site radii calculated from eq. (1) are given in table 1. It can be seen that both $R_A$ and $R_B$ decrease linearly with Mg–Al content ($x$) which can be attributed to the fact that the lattice parameter decreases linearly with $x$ (table 1). The site radius $R_B$ is greater than $R_A$.

In order to determine the cation distributions, X-ray intensity calculations were made using the formula suggested by Buerger [18] and the intensity ratios of planes considered to be sensitive to the cation distribution parameter ($x$) were taken for estimating the cation distributions. Detailed work on such microstructural analysis is reported elsewhere [13]. The ionic configuration based on site preference energy values for individual cations in $Mg_xAl_{2x}Li_{0.5(1-x)}Fe_{2.5(1-x)}O_4$ suggests that $Li^+$ and $Al^{3+}$ ions occupy only B-sites whereas $Mg^{2+}$ and $Fe^{3+}$ ions can occupy both A- and B-sites.

Finally, the cation distribution for these compounds estimated from X-ray intensity calculations and magnetization measurements at 77 K [12] are as follows:

$$x = 0.0 \quad (Fe_{1.0})^A[Li_{0.5}Fe_{1.5}]^B O_4^{-2},$$
$$x = 0.2 \quad (Mg_{0.16}Fe_{0.84})^A[Li_{0.40}Al_{0.40}Mg_{0.04}Fe_{1.16}]^B O_4^{-2},$$
$$x = 0.5 \quad (Mg_{0.42}Fe_{0.58})^A[Li_{0.25}Al_{1.00}Mg_{0.08}Fe_{0.67}]^B O_4^{-2},$$
$$x = 0.6 \quad (Mg_{0.46}Al_{0.07}Fe_{0.47})^A[Li_{0.20}Al_{1.13}Mg_{0.14}Fe_{0.53}]^B O_4^{-2},$$
$$x = 0.7 \quad (Mg_{0.50}Al_{0.14}Fe_{0.36})^A[Li_{0.15}Al_{1.26}Mg_{0.20}Fe_{0.39}]^B O_4^{-2}. \tag{2}$$

Ferrites possess the structure of mineral spinel ($MgAl_2O_4$) that crystallizes in the cubic form with space group Fd3m-Oh$^7$ [5]. It is generally known that the

spinel ferrites exhibit four IR active bands, designated as $\nu_1$, $\nu_2$, $\nu_3$, and $\nu_4$. The occurrence of these four bands has been rationalized on the basis of group theoretical calculations employing space group and point symmetries, both in normal and inverse spinels.

The room temperature (300 K) infrared spectra for $Mg_xAl_{2x}Li_{0.5(1-x)}$ $Fe_{2.5(1-x)}O_4$ system with $x = 0.0$, 0.2, 0.5, 0.6, and 0.7 are shown in figures 1 and 2. It can be seen from the figures that the IR spectrum of magnesium and aluminium co-substituted lithium ferrites are found to exhibit two bands in the range 400–700 cm$^{-1}$. No absorption bands were observed above 700 cm$^{-1}$. The high frequency band $\nu_1$ is in the range 580–640 cm$^{-1}$ and the lower frequency band $\nu_2$ is in the range 460–480 cm$^{-1}$. These bands are common features of all the ferrites [1]. According to Waldron's classification [1] the vibrations of the unit cell of cubic spinel can be constructed in the tetrahedral (A-) site and octahedral (B-) site. So, the absorption band $\nu_1$ is caused by the stretching vibration of the tetrahedral metal–oxygen bond, and the absorption band $\nu_2$ is caused by the metal–oxygen vibrations in octahedral sites. The band positions for all the compositions are given in table 2. The shifting of bands towards high frequency is attributed to the decrease in the unit cell dimension (table 1) and the substitution of lighter cations, $Mg^{2+}$ and $Al^{3+}$ for $Fe^{3+}$ in the system [19]. The nature and the position of bands in $Li_{0.5}Fe_{2.5}O_4$ ($x = 0.0$) are consistent with literature [11]. The shift in band positions is observed as a function of content ($x$). The change in the band position is expected because of the difference in the $Fe^{3+}$–$O^{2-}$ distances for the octahedral and tetrahedral complexes. It was found that Fe–O distance of A-site (1.89 Å) is smaller than that of the B-site (1.99 Å) [20]. This can be interpreted by the more covalent bonding of $Fe^{3+}$ ions at the A-sites than B-sites. The centre frequency of the bands $\nu_1$ and $\nu_2$ show a small variation and they shift slightly towards higher frequency side for $x = 0.0$–0.7 (table 2). It is known that decrease in site radius (table 1) enhances the fundamental frequency and therefore the centre frequency should shift towards higher frequency side. The $\nu_3$ band which arises due to di-
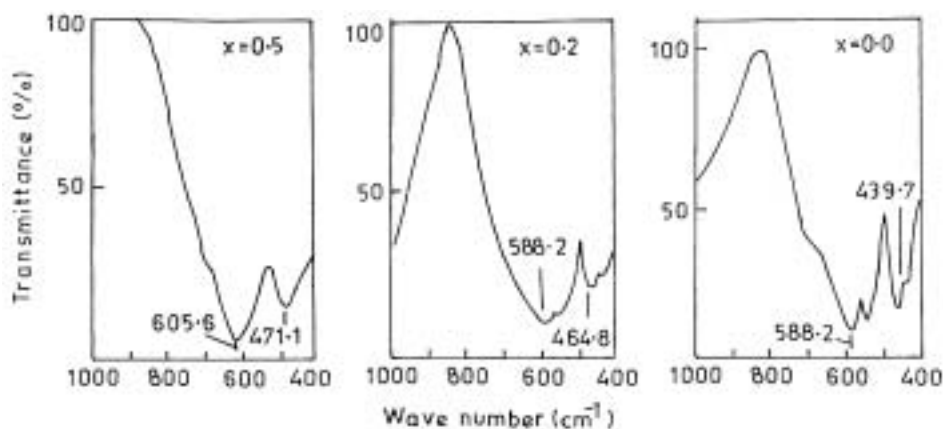


**Figure 1.** Infrared spectra of Mg–Al–Li–Fe–O system with $x = 0.0, 0.2$ and 0.5 samples.

valent metal ion–oxygen complexes in the B-sites and the $\nu_4$ band which depends upon the mass of vibrating divalent tetrahedral cation [19] appears generally below 400 cm$^{-1}$ [7,11,12] and hence they were not observed in the study.

It is important to note that on increasing Mg–Al content ($x$) in the system, bands become more and more broader (figures 1 and 2). The broadening of bands has been reported earlier by many workers [6–11]. Bellad *et al* [11] have observed an increase in broadening for higher content of cadmium in the case of Li–Cd ferrites. They have reported that such broadening is commonly observed in normal spinel ferrites and have attributed it to the statistical distribution of Fe$^{3+}$ ions on A- and B-sites. In the present case, system transfers from inverse Li$_{0.5}$Fe$_{2.5}$O$_4$ ($x = 0.0$) to normal (MgAl$_2$O$_4$) ($x = 1.0$) spinel structure as confirmed by cation distribution formulae (eq. (2)), results in broadening of bands. Furthermore, the intensity of bands is found to decrease with increase in content ($x$) (figures 1 and 2). The decrease in intensity and increase in broadness are explained on the basis of cation distribution formula (eq. (2)). It can be seen that the occupancy ratio of Li : Fe is 1 : 3 on the octahedral site for unsubstituted ferrite (Li$_{0.5}$Fe$_{2.5}$O$_4$; $x = 0.0$). As the content of Mg–Al increases, Mg$^{2+}$ and Al$^{3+}$ ions consistently replace Fe$^{3+}$ ions
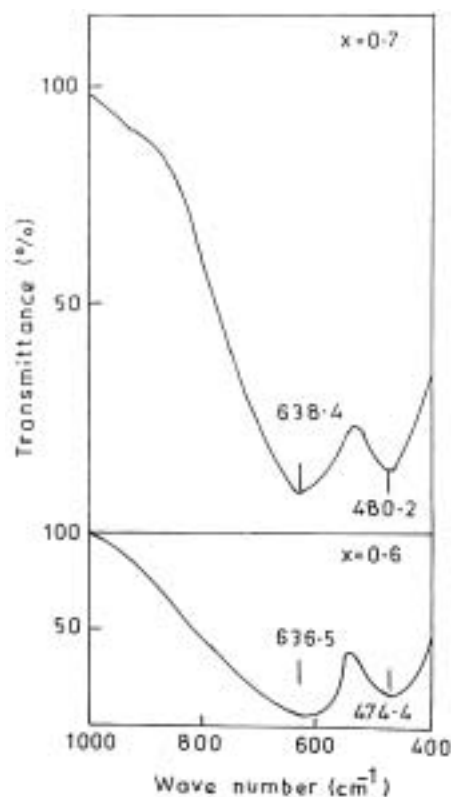


**Figure 2.** Infrared spectra of Mg–Al–Li–Fe–O system with $x = 0.6$ and 0.7 samples.

**Table 2.** Position of IR absorption bands ($\nu_1$, $\nu_2$), bulk modulus ($B$) and velocity ($V_l$, $V_s$), Néel temperature ($T_N$), magneton number ($n_B$) and resistivity ($\rho$) for Mg–Al–Li–Fe–O system.

| Content ($x$) | $\nu_1$ (cm$^{-1}$) | $\nu_2$ (cm$^{-1}$) | $B \times 10^{12}$ (dyne/cm$^2$) | $(V_l = V_s) \times 10^5$ (cm/s) | $T_N$ (K) | $n_B$ ($\mu_B$) | $\log \rho (\log \Omega \cdot \text{cm})$ (363 K) |
|---|---|---|---|---|---|---|---|
| 0.0 | 588.2 | 468.7 | 1.49 | 5.63 | 970 | 2.50 | 5.22 |
| 0.2 | 588.2 | 464.8 | 1.35 | 5.50 | 787 | 1.56 | 5.72 |
| 0.5 | 605.6 | 471.1 | 1.22 | 5.47 | 502 | 0.44 | 8.61 |
| 0.6 | 636.5 | 474.4 | 1.20 | 5.52 | 477 | 0.29 | 10.25 |
| 0.7 | 638.4 | 480.2 | 1.14 | 5.43 | 350 | 0.13 | 8.60 |

from A- and B-sites. At the same time Li$^+$ ions on octahedral site decrease by $(1-x)$. This disturbs the 1 : 3 order to 1 : 2.6 on the octahedral site with increase in Mg–Al content ($x$). This gives rise to a type of chemical disorder on octahedral site, i.e., the stastical distribution of Fe$^{3+}$ ions in B-sites. The disordered systems give rise to broad bands in their IR spectrum [21,22]. Thus, it can be concluded that increase in Mg–Al ions leads to more disordered state.

The close examination of IR spectra revealed the splitting of the principal bands for samples with $x = 0.0$ and 0.2, and is attributed to the Fe$^{2+}$ ion induced Jahn–Teller distortion in the lattice due to a non-cubic component of the crystal field potential, unlike Fe$^{3+}$ ions which do not produce any such effect [23]. The decrease in intensity of shoulders and their complete disappearance for $x > 0.2$, suggest that Fe$^{2+}$ ion formation has been hampered by increase in Mg–Al content and only the $\nu_1$ and $\nu_2$ bands are exhibited. This is also reflected in the high resistivity values for $x > 0.2$ (table 2).

The force constant is a second derivative of potential energy with respect to the site radius, the other independent parameters being kept constant. The force constants, for tetrahedral site ($K_t$) and octahedral site ($K_o$), were calculated employing the method suggested by Waldron [1]. According to Waldron, the force constants $K_t$ and $K_o$ for respective sites are given by

$$K_t = 7.62 \times M_1 \times \nu_1^2 \times 10^{-3},$$
$$K_o = 10.62 \times 10^{-3} \times M_2/2 \times \nu_2^2,$$

where $M_1$ and $M_2$ are the molecular weights of cations on A- and B-sites, respectively.

The variation of force constants with Mg–Al content ($x$) is shown in table 1. The force constants are found to decrease with $x$, and this suggests weakening of interatomic bonding. These results are in contrast with our earlier results on structural properties of Mg$_x$Al$_{2x}$Li$_{0.5(1-x)}$Fe$_{2.5(1-x)}$O$_4$ system [13]. It was found that both, interionic distances between the cation–anion and between cations decrease with increasing content ($x$), resulting in the enhancement of strength of interatomic bonding. Since the IR spectroscopy can give an idea about the change of the molecular structure of the ferrite due to the perturbation occurring in Fe–O bond by introducing Mg$^{2+}$ and Al$^{3+}$ ions the conditions for the formation of weaker

Fe–O bonds can be understood. In other words, the electronic distribution of Fe–O bonds is greatly affected when $Mg^{2+}$ and $Al^{3+}$ ions are introduced in $Li_{0.5}Fe_{2.5}O_4$.

The most conventional technique for bulk modulus, other elastic moduli and Debye temperature determination is the ultrasonic pulse transmission (UPT) technique but informations regarding parameters like force constant, molar heat capacity etc. cannot be obtained from the same. For such purposes IR spectral analysis is found to be superior as it can give an idea about those parameters, which could not be obtained with UPT technique [24,25].

The bulk modulus ($B$) of solids in terms of stiffness constants is defined as $B = 1/3[C_{11} + 2C_{12}]$ [24], but according to Waldron [1] $C_{11} = C_{12}$ and thus $B$ is simply given by $C_{11}$. Further, force constant ($K$) is a product of lattice constant ($a$) and stiffness constant $C_{11}$ [26]. The values of lattice constant obtained from X-ray diffraction analysis and average force constant ($K = (K_t + K_o)/2$) (table 1) from the IR spectral analysis of $Mg_xAl_{2x}Li_{0.5(1-x)}Fe_{2.5(1-x)}O_4$ system have been used for the determination of $B$ and the same are included in table 2. The values of bulk modulus ($B$) are in the same order to those reported for Mn–Zn and Ni–Cd [24] spinel ferrite systems obtained from UPT technique. This suggests validity of the present technique. It is seen that $B$ decreases with increasing Mg–Al content ($x$). The observed decrease in $B$ with $x$ suggests weakening of the interatomic bonding. Similar results have been reported for Ni–Zn [26] and Ni–Cd [24] ferrite systems. These results are consistent with results derived from force constants determination. We have also determined the values of compressional or longitudinal velocity ($V_l$) and shear velocity ($V_s$) using the formula suggested by Waldron [1]: $V_l = (C_{11}/\rho)^{1/2}$ and $V_s = [(C_{11} + C_{12})/2\rho]^{1/2}$ (with $V_l = V_s$) where $\rho$ is X-ray density (table 1). The values of $V_l$ and $V_s$ are also in the same order obtained from IR spectra analysis [1] and ultrasonic pulse transmission technique [24,25] and are summarized in table 2.

Attempt has been made to explain magnetic and electrical behaviour of $Mg_xAl_{2x}Li_{0.5(1-x)}Fe_{2.5(1-x)}O_4$ system in light of structural and optical properties. The weakening in the interatomic bonding should result in decrease in the Néel temperature ($T_N$), as the Néel temperature depends on the active magnetic linkages per magnetic ion per formula unit [25]. Our recent results on magnetic properties of the system show that there is a fast decrease in $T_N$, deduced from thermal variation of AC susceptibility, with $x$ (table 2). This may be due to the weakening in the strength of magnetic interactions as well as due to the decreasing $Fe^{3+}$–$O^{2-}$–$Fe^{3+}$ superexchange linkages resulting from simultaneous replacement of magnetic $Fe^{3+}$ (5 $\mu_B$) by non-magnetic $Mg^{2+}$ and $Al^{3+}$ (0 $\mu_B$) in the spinel lattice. Furthermore, decrease in $T_N$ with $x$ displaying reduction in the ferrimagnetic ordering is in agreement with the magnetization data [12] (table 2).

The resistivity values measured at 363 K by using digital insulation meter are summarized in table 2. The general trend is observed of increasing resistivity value (except for $x = 0.7$) with Mg–Al content ($x$). It is known that in a magnetically ordered system, charge carriers required less energy as compared to disordered system for the conduction process. The present results suggest that on substitution of Mg–Al for Li and Fe in $Mg_xAl_{2x}Li_{0.5(1-x)}Fe_{2.5(1-x)}O_4$ system, weakening in interatomic bonding takes place. In other words, system becomes disordered and as a result resistivity value increases with increasing $x$.

## 4. Conclusions

The summing up of infrared spectral studies suggests the weakening of interatomic bonding on Mg–Al substitution in lithium ferrite, supported by the decrease in force constants, bulk modulus and increase in resistivity value. The bulk modulus, longitudinal and shear velocity values can be determined from an alternative and simple method based on infrared spectral analysis. The nature of absorption bands in infrared spectra depends on the distribution and the type of cations among the tetrahedral and octahedral sites.

## References

[1] R D Waldron, *Phys. Rev.* **99**, 1727 (1955)
[2] A Chim, Seminars, *Ann. Chem.* **7**, 9 (1974)
[3] W L Konijnenijk, *Philos. Res. Rep. Suppl.* **1**, 30 (1975)
[4] J Preudhomme, *Ann. Chim.* **9**, 31 (1974)
[5] W B Whike and B A De Angelis, *Spectrochim. Acta* **A23**, 985 (1967)
[6] K B Modi, K H Jani and H H Joshi, *Acta Ciencia Indica* **25**, 5 (1999)
[7] O S Josyula and J Sobhanadri, *Phys. Status Solidi* **A65**, 479 (1981)
[8] B P Ladgaonkar, C B Kolekar and A S Vaingankar, *Bull. Mater. Sci.* **25**, 351 (2002)
[9] U N Trivedi, K H Jani, K B Modi and H H Joshi, *J. Mater. Sci. Lett.* **19**, 1271 (2000)
[10] D Ravinder, *Mater. Lett.* **40**, 205 (1999)
[11] S S Bellad, R B Pujar and B K Chougule, *Indian J. Pure Appl. Phys.* **36**, 598 (1998)
[12] G J Baldha, K G Saija, K B Modi, H H Joshi and R G Kulkarni, *Mater. Lett.* **53**, 233 (2002)
[13] K B Modi, J D Gajera, M C Chhantbar, K G Saija, G J Baldha and H H Joshi, *Mater. Lett.* **57**, 4049 (2003)
[14] C G Whinfrey, D W Eckart and A Tauber, *J. Am. Chem. Soc.* **82**, 2695 (1960)
[15] B D Cullity, *Elements of X-ray diffraction* (Addison-Wesley Press, Reading, MA, 1959)
[16] S C Watawe, Ph.D. Thesis, Kolhapur University, Kolhapur, India, 2000
[17] K J Standly, *Oxide magnetic material* (Clarenden Press, Oxford, 1972)
[18] M J Buerger, *J. Crystal structure analysis* (Wiley, New York, 1960)
[19] P Tarte and J Preudhomme, *Spectrochim. Acta* **A27**, 1817 (1971)
[20] B J Evans and S Hafner, *J. Phys. Chem. Solids* **29**, 1573 (1968)
[21] M A Amer, M A Ahmed, M K El-Nimr and M A Mostafa, *Hyperfine Interactions* **96**, 91 (1995)
[22] S A Patil, S M Otari, V C Mahajan and A B Patil, *Solid State Commun.* **78**, 39 (1991)
[23] P V Reddy and V D Reddy, *J. Magn. Magn. Mater.* **136**, 279 (1994)
[24] D Ravinder and T Alivea Manga, *Mater. Lett.* **41**, 254 (1999); **37**, 51 (1998)
[25] D Ravinder, K Vijayakumar and B S Boyanov, *Acoustics Lett.* **21**, 30 (1997)
[26] S L Kakani and C Hemrajani, *Text book of solid state physics* (Sultan Chand & Sons, New Delhi, 1997)